Desalination and Water Treatment
www.deswater.com

doi:10.5004/dwt.2018.22262

113 (2018) 179–186
May

Electrochemical synthesis of ferrate(VI): optimization of parameters and evaluation of their impact in production cost

Javier Quino-Favero[a,*], Raúl Eyzaguirre[a], Paloma Mogrovejo[a], Patricia Prieto[a], Lisveth Flores del Pino[b]

[a]*Instituto de Investigación Científica, Universidad de Lima, Avenida Javier Prado Este 4600, Lima, Perú, email: jquinof@ulima.edu.pe (J. Quino-Favero), reyzagui@ulima.edu.pe (R. Eyzaguirre), mogrovejopaloma@gmail.com (P. Mogrovejo), paty.mpv@gmail.com (P. Prieto)*
[b]*Departamento de Química, Universidad Nacional Agraria La Molina, Avenida La Molina S/N, email: lisveth@lamolina.edu.pe (L.F. del Pino)*

Received 5 April 2017; Accepted 26 March 2018

ABSTRACT

Ferrates have attracted considerable research in the last few decades because their activity is not associated with toxic byproducts. This research investigated the effect of three factors on ferrate (VI) synthesis using an electrochemical reactor: electrolyte concentration, current density, electrode effective surface: electrolyte volume ratio (S/V ratio). The results of ferrate(VI) production using two different membranes were compared. Electrolyte concentration had the greatest effect on ferrate(VI) production. Ferrate(VI) concentration of 250 mmol dm^{-3} was achieved using 20 mol dm^{-3} of NaOH electrolyte, current density of 80 Am^{-2}, and 2.21 S/V_{An} during five hours of electrolysis. A cost analysis of the consumable components such as the electrolyte, electric energy, and dissolved iron demonstrated that the electrolyte concentration had the greatest influence.

Keywords: Ferrate(VI); Electrochemical reactor; Membrane; Production cost; S/V ratio

1. Introduction

Ferrate species are non-stable forms of oxidized iron that show high oxidizing activity, even higher than ozone under acidic conditions [1]. Ferrate(VI) ions are also active at circumneutral pH, albeit with a lower oxidizing capacity [2]. Owing to these properties, ferrates can oxidize metals and metalloids, decompose a wide variety of organic compounds, remove COD and phosphorus, and kill or inactivate bacteria, viruses, and other microorganisms [3–5].

Ferrate species are considered "green oxidants" because their activity, unlike chlorine agents activity, is not associated with toxic byproducts [2,6–8] or genotoxicity [9]. In an aqueous solution, ferrate(VI) reduces itself rapidly by oxidizing other substances/microorganisms to produce ferric ions. These ions act as coagulating agents that co-precipitate with the oxidized compounds and leave some harmless ferric ions in the solution.

Recently, ferrate(VI) has attracted interest for treating contaminants of emerging concern [10]. Very small amounts of ferrate(VI) are needed to decompose substances such as antibiotics, hormones, and anti-inflammatory drugs [11,12] that otherwise pass through traditional water treatment systems without being transformed or inactivated significantly.

Three methods have been reported to produce ferrates: wet synthesis, dry synthesis, and electrochemical synthesis [13]. Of these, electrochemical synthesis has been studied the most because it is economical and relatively easy for direct application in on-line processes [14]. Ferrate(VI) production by the electrochemical method and dosage in-situ make the storage of ferrate(VI) unnecessary, thus preventing its decomposition [15,16]. However, a drawback of the direct application of the ferrate(VI) produced by the electrochemical method is that it could considerably increase

*Corresponding author.

water pH levels because ferrate(VI) needs a concentrated hydroxide solution to be produced in high yields [17]. Thus it is necessary to know the conditions under which the ratio $[FeO_4]^{2-}$:[NaOH] is the highest while its production cost is the lowest.

Several parameters influence ferrate(VI) electrochemical production: anode type and composition, electrolyte concentration, current density, and temperature. Anode composition will determine its velocity of dissolution as well as the characteristics of the oxide layer that forms over the electrode surface which in turn impacts production efficiency [18]. Electrolyte concentration has a critical role in ferrate(VI) stability; higher electrolyte concentrations decreases and inhibit the redox reaction of ferrate(VI) with water due to lower free water activity [19,20]. Current density selection must consider the following: a high potential favors the parasitic reaction of oxygen evolution that competes with ferrate(VI) production whilst a low potential enhances the formation of intermediates which limits the ferrate(VI) yield [21]. Finally, increasing the temperature retards the oxide layer formation in the anode enhancing its dissolution and hence, ferrate(VI) production. However, it is not so simple, since too high temperature leads to efficiency decrease because of ferrate(VI) decomposition [22].

Of the aforementioned parameters, this research evaluated the effects of electrolyte concentration and current density because the electrolyte and the energy are the most expensive components. Adding to these, we evaluated the electrode effective surface: electrolyte volume ratio (S/V ratio) in a divided cell to assess to what extent it could be possible to obtain a more concentrated ferrate(VI) solution using thinner chambers. One extra membrane type was also tested to explore its potential effect for ferrate(VI) production as little research has been done on the subject. Parameter values for ferrate(VI) synthesis were selected based on previous experiences reported in the literature [21,23–25].

Furthermore, costs were broken down to identify the factor (electrolyte, electric energy, or dissolved iron) that most impacted on the production cost. Production cost analysis of all these components was used to determine the feasibility for a specific application. To the best of our knowledge, only one other study has addressed this issue [26]. This analysis showed that energy consumption and/or faradic efficiency as sole parameters did not always lead to cost-effective conditions because energy had little effect on the total ferrate(VI) production cost.

2. Experimental

2.1. Reactor assembly

The electrochemical reactor (Fig. 1) was made of polymethylmethacrylate (PMMA) and had two chambers that were separated by a 5 cm × 5 cm membrane. The cathode (5 cm × 5 cm) was made of graphite and the anode (5 cm × 5 cm), of low-carbon steel whose composition was determined by mass spectrometry using a Spectro 1 Spectrolab M8 arc spark optical emission spectrometer (Table 1). Anode composition corresponded to the anode surface without any pre-treatment. The electrodes were positioned vertically and parallel to each other. The separation distance between each electrode and the membrane defined the chamber volumes; for separation distances of 5, 4, and 3.5 mm, the effective volumes of a single chamber were 15.8, 12.8, and 11.3 cm^3, respectively. Thus, the total gap between electrodes varied from 7 to 10 mm. The separation distances were varied using separating plates made of PMMA and of different widths. The effective electrode area (S) and the effective volume (V) of the chamber defined the S/V values; a 5 mm separation corresponded to S/V ratio of 1.58

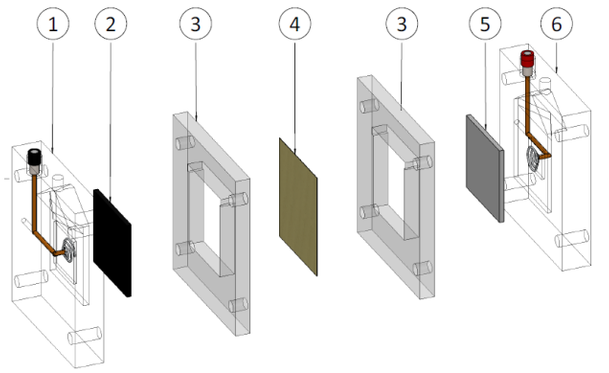

Fig. 1. Schematic of electrochemical reactor. 1: connection plate (negative), 2: cathode, 3: separating plates, 4: membrane, 5: anode, and 6: connection plate (positive). Width of separating-plates is exaggerated for clarity.

Table 1
Composition of iron anode used in this study

Compound	wt%
C	0.0470
Cr	0.0206
Cu	0.0110
Zr	< 0.01
Si	0.0545
Mo	< 0.01
Nb	< 0.01
B	< 0.01
Mn	0.1283
Ni	0.0127
Ti	0.0010
N	0.0063
P	0.0124
Al	0.0185
V	< 0.01
O	0.0204
S	0.0062
Co	< 0.01
W	< 0.01
Fe	99.65

cm^{-1}; a 4 mm separation corresponded to S/V ratio of 1.95 $cm^{-1}$and, a 3.5 mm separation corresponded to S/V ratio of 2.21 cm^{-1}. The S/V ratios tested were conditioned by the reactor design and assembly.

The membranes tested were CTIEM-1 (Perfluorosulfonic Acid Cation Exchange Membrane Zibo Cantian, China) which is used as an ion exchange membrane for chlor-alkali industry (2.3 Ω cm^2, pore diameter <100 nm according FSEM measurements), and Zirfon Perl UTP 500 (Agfa, Germany), which is used for alkaline electrolysis and characterized by its low ionic resistance and low pore diameter (≤0.3 Ω cm^2 at 30°C, in 30 wt% KOH solution, pore diameter <0.15 μm).

2.2. Ferrate(VI) production

A regulated DC power supply (BK Precision 1740) operated under a constant current regime was used. Three different electric currents, 100, 150, and 200 mA, corresponding to current densities of 40, 60, and 80 A m^{-2}, were tested. The applied potential difference and electric current values were measured using two multimeters (Fluke 175) connected in parallel and serial modes, respectively. Both reactor chambers were loaded with the same NaOH concentration (8, 10, 12, 14, 16, 18, and 20 mol dm^{-3}) to test ferrate(VI) production. Iron electrodes were cleaned before each experiment using sandpaper.

25-μL samples of the anolyte were taken each hour during the total electrolysis time of five hours, diluted in the same electrolyte, and measured immediately. The ferrate(VI) produced was measured by visible spectroscopy using a Perkin-Elmer Lambda 40 UV/Vis spectrophotometer, and the ferrate(VI) ion concentration was calculated as

$$\left[FeO_4\right]^{2-} = \frac{\Delta_{Abs} V_{final}}{\varepsilon \ell V_{sample}} \quad (1)$$

where Δ_{Abs} is the difference of extinctions with the blank, measured at 505 nm, V_{final} is the sum of the sample volume (V_{sample}) and the solution volume added for dilution, ε is the reported molar extinction coefficient of ferrate(VI)(1050 $dm^3\ mol^{-1}\ cm^{-1}$) and l is the cell path (1 cm). The faradic efficiency was calculated as

$$Efficiency = \frac{Ferrate(VI)_{experimental}}{Ferrate(VI)_{theoretical}} \times 100 \quad (2)$$

with

$$Ferrate(VI)_{theoretical} = \frac{Mlt}{zF} \quad (3)$$

where M is the ferrate(VI) molar mass (g), is the applied current (A), t is time (s), z is the number of electrons transferred (=6), and F is the Faraday constant (96485 $Cmol^{-1}$).

Temperature was monitored with a K type thermocouple and all testing was carried out at 25°C. After an electrolysis time of five hours, the temperature increase did not exceed 1°C when working with current densities of 40 and 60 A m^{-2} and did not exceed 2°C when working with 80 Am^{-2}.

The ferrate(VI) production rate was obtained by fitting a simple linear regression for ferrate(VI) production over time during the five hours of electrolysis. The coefficient of determination (0.898–0.999) suggested that the goodness of fit was very good for all electrolyte concentrations tested, thus strongly supporting the assumption of constant production rate. Rates calculated were used to build the polynomial curve in Fig. 2.

The energy expenditure was obtained by calculating the area under the curve of the power (measured in VA) vs. time during the five hours of electrolysis. No further data is reported after this time because ferrate(VI) production rate began to decrease departing from linearity.

The energy cost (0.0784 US$ $kW^{-1}h^{-1}$) was obtained from a provider of low-tension power in Lima, the price of NaOH (0.59 US$ kg^{-1}) and the price of low-carbon steel (1.10 US$ kg^{-1}) were obtained from the local providers Quimpac S.A. and Polimetales S.A.C respectively. Anode consumption was calculated using Faraday's law and the total anodic charge considering the transference of two electrons, which is the minimum number of electrons that causes anode dissolution.

2.3. Statistical analysis

All statistical analyses were performed using the software R [27]. To evaluate the relation between the electrolyte concentration and the ferrate(VI) production, cubic polynomial models were fitted. To evaluate the effects of the electrolyte concentration and current density, anode and cathode S/V ratio, membrane type and current density on ferrate(VI) production, a linear model was fitted considering both factors and their interaction in each case. In all three cases, analysis of variance tables were computed to evaluate the significance of the factors.

3. Results and discussion

3.1. Effect of electrolyte concentration and current density on ferrate(VI) production

Experiments were performed with a CTIEM-1 membrane, with an anode S/V ratio of 1.58 cm^{-1} and cathode S/V of 1.95 cm^{-1}. The results showed that increasing electrolyte concentration increased the production rate; the maximum ferrate(VI) production rate for the three current densities was obtained with a sodium hydroxide concentration of 20 mol dm^{-3}, as in a previous study [25]. Curves of the ferrate(VI) production rate per hour versus the electrolyte concentration were adjusted to a cubic polynomial model for each current density (Fig. 2). The coefficients of determination (0.967, 0.998, and 0.9474 at 40, 60, and 80 A m^{-2}, respectively) indicate that the cubic models well fit the data. The cubic models allowed us to find inflection points; in this case, these are points where the increments in the ferrate(VI) production rate change from increasing to decreasing with an additional unit of electrolyte concentration. In this experiment, the inflection points were 15.365, 14.7708, and 13.8249 mol dm^{-3} for 40, 60, and 80 A m^{-2}, respectively, suggesting that concentrations of at least these values should be used. The same approach was used for faradic efficiencies (Fig. 3), where all inflection points were greater than 14 mol dm^{-3}. Thus, as a rule, we recom-

mend using at least 14 mol dm^{-3} irrespective of the current density for any application.

The differences in ferrate(VI) production rates at increasing current densities tested are small (Fig. 2), even though it was expected higher production rates with higher current densities. This is not the case because efficiency drops at higher current density values (Fig. 3).

These results were consistent with a previous study [28] and led us to use 40 A m^{-2} for the next set of experiments. However, the effect of current density on ferrate(VI) production was reevaluated when the S/V ratios were changed (Section 3.3).

To quantify the magnitude of the effect of each variable, an analysis of variance was performed. Table 2 shows the results for a linear model with current density and electrolyte concentration as explanatory variables and ferrate(VI) production as the response. The sum of squares shows that almost all observed variability in the ferrate(VI) production at the fifth hour is explained by the NaOH concentration (98% for NaOH concentration, 1.46% for interaction, and 0.49% for the current density).

Table 2
Analysis of variance for the effect of current density (j), electrolyte concentration (NaOH), and current density and electrolyte concentration interaction (NaOH:j) on ferrate(VI) production

Factor	DF	SS	MS	F	p
NaOH	6	92434	15406	7197.88	0.0000
j	2	459	230	107.30	0.0000
NaOH:j	12	1381	115	53.79	0.0000
Residuals	21	45	2		

DF: Degrees of Freedom; SS: Sums of Squares; MS: Mean Squares; F: F statistical value; p: Probability value.

3.2. Effect of the S/V ratio on ferrate(VI)concentration

The S/V ratio expresses the relation between the electrode surface and the volume of electrolyte in the chamber [22–24]. Two membranes (CTIEM-1 and Zirfon) were evaluated at 40 A m^{-2}, 20 mol dm^{-3} NaOH, using 2.21 cm^{-1} and

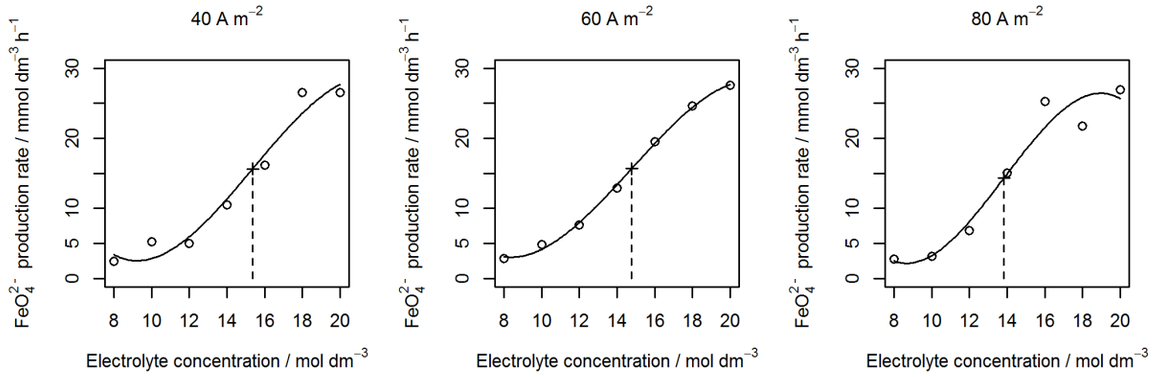

Fig. 2. Cubic polynomial models fitted for ferrate(VI) production rates versus electrolyte concentration at three current densities. Inflection points are marked with vertical lines. The membrane used was CTIEM-1 with anode S/V ratio of 1.58 cm^{-1} and cathode S/V ratio of 1.95 cm^{-1}.

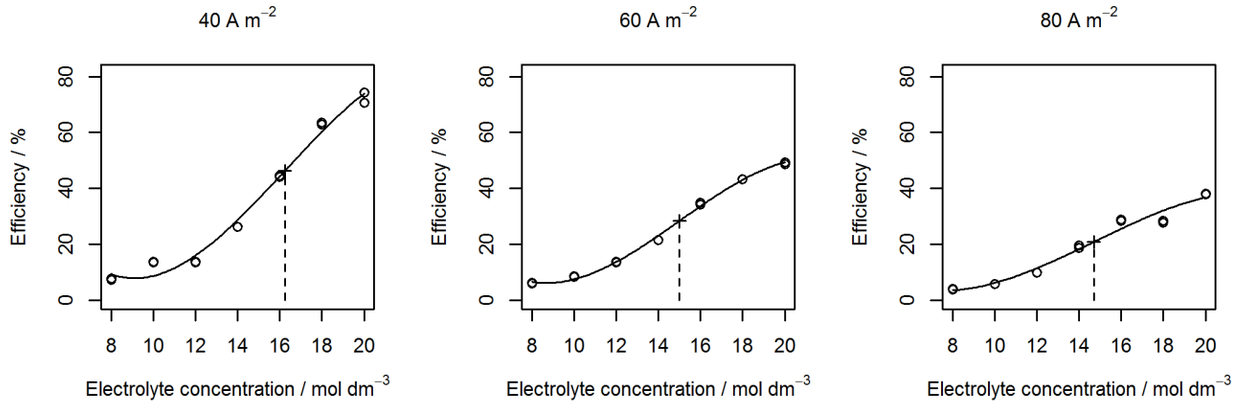

Fig. 3. Cubic polynomial models fitted for faradic efficiency versus electrolyte concentration at three current densities. Each point corresponds to the fifth hour of electrolysis. Inflection points are marked with vertical lines. The membrane used was CTIEM-1 with anode S/V ratio of 1.58 cm^{-1} and cathode S/V ratio of 1.95 cm^{-1}.

1.58 cm^{-1} S/V ratios, with two replications, for a total of 16 experiments. In each experiment, the ferrate(VI) molar concentration and total production were determined every hour.

The effect of the S/V_{An} ratio was significant with both membranes (p = 0.0151 and p = 0.0026), but that of S/V_{Ca} was not (p = 0.8757 and p = 0.5310). The sum of squares (Table 3) shows that the variability is explained mainly by the S/V_{An} relation (73.6% and 77.6%), then by the interaction of S/V_{An} and S/V_{Ca} ratios (8.6% and 14.6%), and finally by the S/V_{Ca} (0.1% and 0.8%) for both membranes. Fig. 4 shows that the highest ferrate(VI) concentrations were achieved for 2.21 cm^{-1} S/V_{An} ratio irrespective of the membrane type. These results are in agreement with Sun [24], who reported that the optimum S/V was 1.5–2 cm^{-1} when grey cast iron was used.

Therefore, thinner anode chambers are suggested to realize large ferrate(VI) concentrations. Other studies have also used thinner anode chambers compared to cathode chambers [29,30]. Although it seems logical to further reduce the separation distance between the anode and the membrane, a very short distance would compromise ferrate(VI) synthesis because bubbles produced by oxygen evolution could adhere to the electrode surface and reduce production by interrupting the current flow [21].

Fig. 4 also shows the effect of membrane type on ferrate(VI) obtained concentration. The CTIEM-1 membrane showed better performance than the Zirfon membrane for all the S/V ratios.

3.3. Effect of current density with best S/V_{An} ratio and separating membranes

The effect of varying the current density was tested again to verify that the results found in Section 3.1, where this variable is non-significant, remained the same with the new S/V ratios. Two runs per membrane were carried out at 40 and 80 A m^{-2}, 20 mol dm^{-3} of NaOH, and 2.21 cm^{-1} S/V_{An} and S/V_{Ca} ratios.

Fig. 5 shows the results for ferrate(VI) concentration with each membrane at 40 and 80 A m^{-2}. Ferrate(VI) concentrations up to 250 mmol dm^{-3} were achieved with an increase in the current density, corresponding to a $[FeO_4]^{2-}$:[NaOH] ratio of 0.0125. The analysis of variance

Table 3
Analysis of variance for the effect of anode (S/V_{An}) and cathode (S/V_{Ca}) S/V relation, and anode and cathode S/V relation interaction (S/V_{An}:S/V_{Ca}) on ferrate(VI) concentration with CTIEM-1 and Zirfon membranes

Membrane	Factor	DF	SS	MS	F	p
CTIEM-1	S/V_{An}	1	2163.88	2163.88	16.62	0.0151
	S/V_{Ca}	1	3.62	3.62	0.03	0.8757
	S/V_{An}:S/V_{Ca}	1	253.12	253.12	1.94	0.2357
	Residual	4	520.88	130.22		
Zirfon	S/V_{An}	1	1708.90	1708.90	44.48	0.0026
	S/V_{Ca}	1	18.03	18.03	0.47	0.5310
	S/V_{An}:S/V_{Ca}	1	321.49	321.49	8.37	0.0444
	Residual	4	153.68	38.42		

DF: Degrees of Freedom; SS: Sums of Squares; MS: Mean Squares; F: F statistical value; p: Probability value.

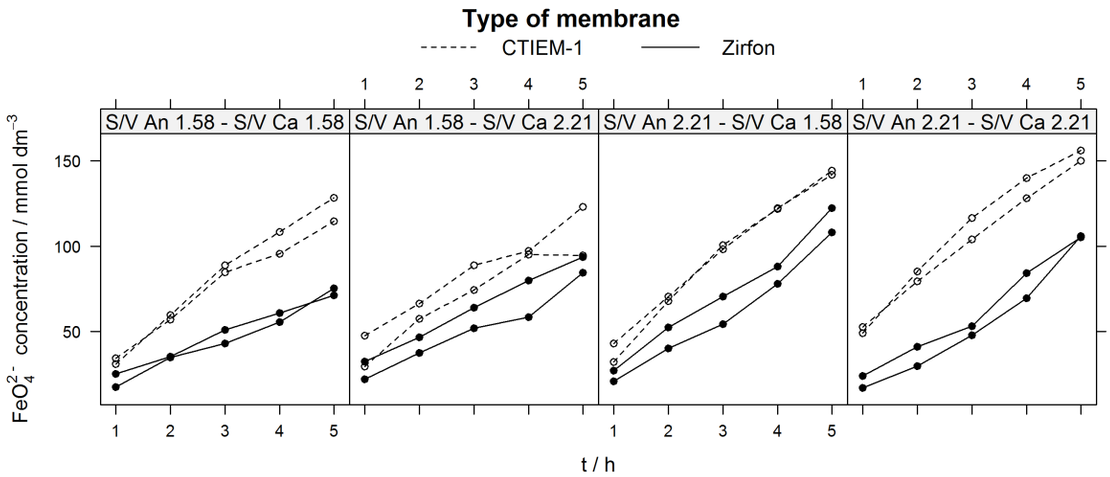

Fig. 4. Ferrate(VI) concentration (mmol dm^{-3}) curves for five hours electrolysis runs at current density of 40 A m^{-2} with different anode and cathode S/V ratios (cm^{-1}), and with two types of membranes.

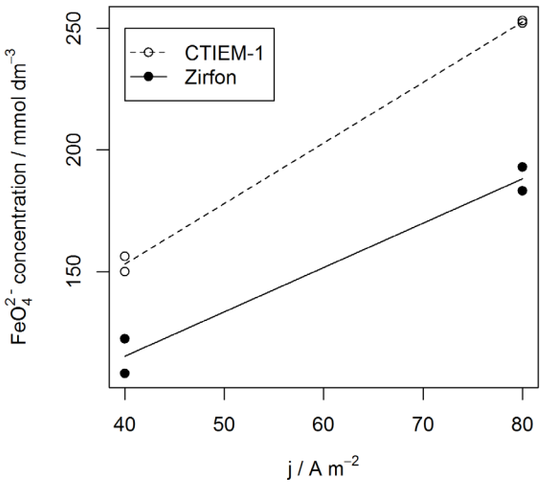

Fig. 5. Ferrate(VI) concentration (mmol dm^{-3}) at the fifth hour of electrolysis with CTIEM-1 and Zirfon membranes and current densities of 40 and 80 A m^{-2}. The anode and cathode S/V ratios were both 2.21 cm^{-1}.

Table 4
Analysis of variance for the effect of membrane type, current density (j), and membrane type and current density interaction (Membrane:j) on ferrate(VI) production

	DF	SS	MS	F	p
Membrane	1	4272.5	4272.5	110.51	0.0005
j	1	16626.3	16626.3	430.04	0.0000
Membrane:j	1	669.5	669.5	17.32	0.0141
Residuals	4	154.6	38.7		

DF: Degrees of Freedom; SS: Sums of Squares; MS: Mean Squares; F: F statistical value; p: Probability value.

table (Table 4) showed significant differences between the use of the two membranes and between both current densities.

There was also a significant interaction between the use of the membrane and the current density but without a crossover effect. This interaction results from the greater production gap between the CTIEM-1 and Zirfon membranes at 80 A m^{-2}.

As S/V values and electrolyte concentration were kept constant with each current density tested, the increase in production gap at higher current density could be the result of the differences of the potential achieved at these conditions. When current density was increased from 40 to 80 A m^{-2} (Fig. 5), the reactor with CTIEM-1 membrane increased its potential 1.44 V while the one with Zirfon membrane experienced a slight increase of 0.14 V. To verify if the lower potential developed while using the Zirfon membrane explained its lower performance, a nitrile mask was used to reduce the membrane area, thus increasing the potential due to a reduction of the interfacial area. Table 5 shows higher ferrate(VI) concentrations when potential increased for the Zirfon membrane due to the small areas used.

Table 5
Ferrate(VI) concentrations (mmol dm^{-3}) at the fifth hour at increasing potentials and constant current density with Zirfon membrane. S/V_{An} ratio 2.78 cm^{-1} and NaOH 20 mol dm^{-3}

Membrane	Area cm^2	Potential V	Current density A m^{-2}	Ferrate(VI) mmol dm^{-3} at fifth hour[a]
CTIEM-1	25	4.6	80	287 ± 0.0005
Zirfon	25	2.5		213 ± 0.0030
Zirfon	1.08	3.1		235 ± 0.0099
Zirfon	0.48	3.7		245 ± 0.0044

[a]Average ± standard deviation

3.4. Production cost

The production costs are defined as the sum of the costs of all consumables required for ferrate(VI) production, namely, NaOH electrolyte, electric energy, and dissolved iron.

3.4.1. Effect of electrolyte and current density

As mentioned in Section 3.1, using the maximum electrolyte concentration led to both the highest ferrate(VI) yields and efficiencies. Fig. 6 shows that the lowest costs were achieved at 20 mol dm^{-3}. On the other hand, cost analysis showed that the electrolyte was the main component influencing the ferrate(VI) production cost. When 8 mol dm^{-3} of electrolyte was used, its cost represented 74.24% of the average production cost for the three current densities; dissolved iron represented 15.55% and energy consumption, 3.48%. As the electrolyte concentration increased, log-

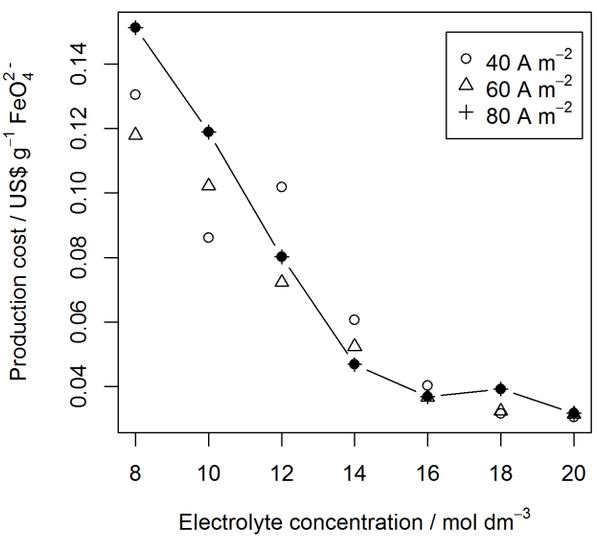

Fig. 6. Electrolyte concentration versus production cost at varying current densities. Solid circles represent the mean for each electrolyte concentration over the three current densities. The anode S/V ratio was 1.95 cm^{-1} and the cathode S/V ratio was 1.58 cm^{-1}.

ically its share of the cost also increased. For example, at 20 mol dm^{-3}, the shares of the cost of the electrolyte, dissolved iron, and energy consumption were 86.66%, 9.99%, and 3.34%, respectively.

As the aim is to achieve the lowest production cost and the electrolyte is the most expensive element, we suggest optimizing the parameters involved in ferrate(VI) production in order to rise the $[FeO_4]^{2-}$:[NaOH] ratio. Maximizing the previous relationship indirectly will result in the lowest production costs, and this approach will eliminate the need for other researchers to perform cost analysis. Additionally, this optimized relationship minimizes the amount of electrolyte added per unit of ferrate(VI) during water treatment, which is essential for avoiding undesired pH changes.

3.4.2. Effect of S/V ratios on production cost

The lowest production cost was achieved in runs that used S/V_{An} of 2.21 cm^{-1} with both membrane types (Fig. 7).This is because ferrate(VI) mass is produced in lesser volume of electrolyte when higher S/V_{An} ratio was used. Lower costs were achieved using the CTIEM-1 membrane than the Zirfon membrane for all treatments.

3.4.3. Effect of current density with best S/V ratios tested on production cost

Increasing the current density resulted in increased ferrate(VI) production for both S/A_{An} and S/V_{Ca} ratios of 2.21 cm^{-1}; doing so also reduced the production cost (Table 6). The lowest cost was achieved at 80 A m^{-2} with the CTIEM-1 membrane. However low faradic efficiency (45.9%) was achieved under these conditions compared with other results obtained in this study. This is because energy expenditure has little impact on the production cost. The fact that the lowest cost of ferrate(VI) production is not associated with the highest faradic efficiency is an important result because it shows that the optimum parameters should not be selected exclusively based on that indicator.

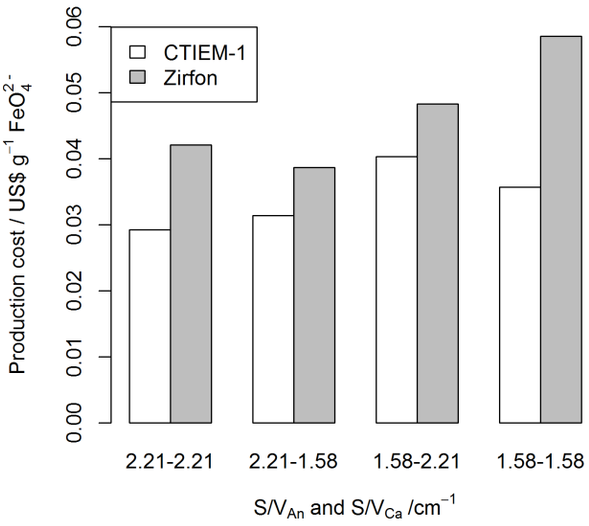

Fig. 7. Production costs of ferrate(VI) for different anode and cathode S/V ratios at current density of 40 A m^{-2}.

Table 6
Production costs and efficiencies for three different combinations of membrane type and current density (j) in A m^{-2}. Both S/V_{An} and S/V_{Ca} ratios fixed at 2.21 cm^{-1}

Membrane	j	US$[a] $g^{-1}FeO_4^{2-}$	Efficiency[a]%
CTIEM-1	40	0.02927 ± 0.00078	55.62 ± 1.59
CTIEM-1	80	0.02014 ± 0.00029	45.90 ± 0.14
Zirfon	80	0.02628 ± 0.00096	34.18 ± 1.26

[a]Average ± standard deviation

4. Conclusions

Cost analysis showed that the electrolyte represents at least 80% of the ferrate(VI) production cost. Nevertheless the use of 20 mol dm^{-3} electrolyte, the maximum possible concentration, resulted in the most cost-effective production in terms of US$ g^{-1} offer rate(VI) because this concentration greatly increased ferrate(VI) production. The maximum $[FeO_4]^{2-}$:[NaOH] ratio was found to be a suitable reference for realizing the lowest production cost. As the lowest production cost of ferrate(VI) is not necessarily associated with the highest faradic efficiency, the optimum production parameters should not be solely based on that indicator.

For both membranes, the observed variability in the ferrate concentration obtained is mainly explained by the S/V_{An} relation, where higher S/V_{An} realized higher ferrate concentrations. S/V_{Ca} was not significant, and accounted for less than 1% of the differences.

The separating membrane, which was not considered in previous studies, is another parameter that could be optimized in the future. In our study, the CTIEM-1 membrane showed superior performance in comparison to the Zirfon membrane, which was expected to yield better due to its low electric resistance; however membrane electrical conductivity produced the opposite effect. Higher pore sizes are associated with higher conductivities [31] and hence to lower potentials. We recommend future optimizations with other membranes and a study of the effect of S/V_{An} ratio and its combined effect with the current density and potential.

Acknowledgments

The Instituto de Investigación Científica de la Universidad de Lima (IDIC) provided the funding for this research under contracts 56.017.2014 and 56.012.2015. The authors are grateful to the University's Computer-Integrated Manufacturing Laboratory for the use of the CNC milling machine and to Fundición Central for the optical emission spectrometer analysis. The authors would like to specially thank graduate student Mario Alarcón and Professor Fabricio Paredes, who contributed greatly to the electrochemical reactor's design and construction.

References

[1] J.-Q. Jiang, B. Lloyd, Progress in the development and use of ferrate(VI) salt as an oxidant and coagulant for water and wastewater treatment, Water Res., 36 (2002) 1397–1408.

[2] D. Tiwari, S.-M. Lee, Ferrate(VI) in the Treatment of Wastewaters: A New Generation Green Chemical, in: F.S. García Einschlag (Ed.), Waste Water - Treat. Reutil., INTECH, 2011: pp. 241–276. http://cdn.intechopen.com/pdfs-wm/14558.pdf.

[3] V.K. Sharma, R. Zboril, R.S. Varma, Ferrates: greener oxidants with multimodal action in water treatment technologies, Acc. Chem. Res., 48 (2015) 182–191.

[4] F. Kazama, Viral inactivation by potassium ferrate, Water Sci. Technol., 31 (1995) 165–168.

[5] J.-Q. Jiang, C. Stanford, A. Mollazeinal, The application of ferrate for sewage treatment: pilot-to full-scale trials, in: Proc. 12th Int. Conf. Environ. Sci. Technol., Rhodes, 2011: pp. A775–A782.

[6] M.-S. Zhang, B. Xu, Z. Wang, T.-Y. Zhang, N.-Y. Gao, Formation of iodinated trihalomethanes after ferrate pre-oxidation during chlorination and chloramination of iodide-containing water, J. Taiwan Inst. Chem. Eng., 60 (2016) 453–459.

[7] V.K. Sharma, F. Kazama, H. Jiangyong, A.K. Ray, Ferrates (iron(VI) and iron(V)): environmentally friendly oxidants and disinfectants, J. Water Health., 3 (2005) 45–58.

[8] B. Darko, J.-Q. Jiang, H. Kim, L. Machala, R. Zboril, V.K. Sharma, Water Reclamation and Sustainability, Elsevier, 2014.

[9] J.-Q. Jiang, H.B.P. Durai, M. Petri, T. Grummt, R. Winzenbacher, Drinking water treatment by ferrate(VI) and toxicity assessment of the treated water, Desal. Water Treat., 57 (2016) 26369–26375.

[10] J.-Q. Jiang, The role of ferrate(VI) in the remediation of emerging micro pollutants, Procedia Environ. Sci., 18 (2013) 418–426.

[11] B. Yang, G.-G. Ying, J.-L. Zhao, S. Liu, L.-J. Zhou, F. Chen, Removal of selected endocrine disrupting chemicals (EDCs) and pharmaceuticals and personal care products (PPCPs) during ferrate(VI) treatment of secondary wastewater effluents., Water Res., 46 (2012) 2194–2204.

[12] J.-Q. Jiang, H.B.P. Durai, R. Winzenbacher, M. Petri, W. Seitz, Drinking water treatment by *in situ* generated ferrate(VI), Desal. Water Treat., 55 (2015) 731–739.

[13] J.-Q. Jiang, Advances in the development and application of ferrate(VI) for water and wastewater treatment, J. Chem. Technol. Biotechnol., 89 (2014) 165–177.

[14] S. Licht, X. Yu, Electrochemical alkaline Fe(VI) water purification and remediation, Environ. Sci. Technol., 39 (2005) 8071–8076.

[15] J.-Q. Jiang, C. Stanford, M. Alsheyab, The online generation and application of ferrate(VI) for sewage treatment—A pilot scale trial, Sep. Purif. Technol., 68 (2009) 227–231.

[16] J.Q. Jiang, C. Stanford, A. Mollazeinal, The application of ferrate for sewage treatment: Pilot-to full-scale trials, Glob. Nest J., 14 (2012) 93–99.

[17] E. Yang, J. Shi, H. Liang, On-line electrochemical production of ferrate (VI) for odor control, Electrochim. Acta., 63 (2012) 369–374.

[18] L. Nikolić-Bujanović, M. Čekerevac, M. Vojinović-Miloradov, A. Jokić, M. Simičić, A comparative study of iron-containing anodes and their influence on electrochemical synthesis of ferrate(VI), J. Ind. Eng. Chem., 18 (2012) 1931–1936.

[19] S. Licht, pH measurement in concentrated alkaline solutions, Anal. Chem., 57 (1985) 514–519.

[20] L. Ding, H. Liang, X. Li, Oxidation of CH3SH by in situ generation of ferrate(VI) in aqueous alkaline solution for odour treatment, Sep. Purif. Technol., 91 (2012) 117–124.

[21] Z. Mácová, K. Bouzek, J. Híveš, V.K. Sharma, R.J. Terryn, J.C. Baum, Research progress in the electrochemical synthesis of ferrate(VI), Electrochim. Acta., 54 (2009) 2673–2683.

[22] M. De Koninck, T. Brousse, D. Bélanger, The electrochemical generation of ferrate at pressed iron powder electrodes: effect of various operating parameters, Electrochim. Acta., 48 (2003) 1425–1433.

[23] M. Alsheyab, J.-Q. Jiang, C. Stanford, Electrochemical generation of ferrate (VI): Determination of optimum conditions, Desalination, 254 (2010) 175–178.

[24] X. Sun, Q. Zhang, H. Liang, L. Ying, M. Xiangxu, V.K. Sharma, Ferrate(VI) as a greener oxidant: Electrochemical generation and treatment of phenol., J. Hazard. Mater., 319 (2016) 130–136.

[25] S. Barişçi, F. Ulu, H. Särkkä, A. Dimoglo, M. Sillanpää, Electrosynthesis of ferrate (VI) ion using high purity iron electrodes: Optimization of influencing parameters on the process and investigating its stability, Int. J. Electrochem. Sci., 9 (2014) 3099–3117.

[26] S. Barışçı, H. Särkkä, M. Sillanpää, A. Dimoglo, The treatment of greywater from a restaurant by electrosynthesized ferrate (VI) ion, Desal. Water Treat., 57 (2015) 11375–11385.

[27] R Core Team, R: A language and environment for statistical computing, R Foundation for statistical computing (2017). Viena, Austria. https://www.r-project.org/.

[28] W. He, J. Wang, C. Yang, J. Zhang, The rapid electrochemical preparation of dissolved ferrate(VI): Effects of various operating parameters, Electrochim. Acta., 51 (2006) 1967–1973.

[29] Z. Ding, C. Yang, Q. Wu, The electrochemical generation of ferrate at porous magnetite electrode, Electrochim. Acta., 49 (2004) 3155–3159.

[30] H. Wang, Y. Liu, F. Zeng, S. Shuang, Electrochemical synthesis of ferrate (VI) by regular anodic replacement, Int. J. ElectroChem. Sci., 10 (2015) 7966–7976.

[31] J. Encinas, M. Castillo-Ortega, F. Rodríguez, V.M. Castaño, Preparation of electrically conductive polymeric membranes, J. Elec. Mater., 44 (2015) 3225.